Journal of Applied Polymer Science

Transparency and water vapor barrier properties of polybenzoxazine-silica nanocomposites provided with perhydropolysilazane

Joo Yeon Lee, Reiko Saito
Department of Chemical Science and Engineering, Tokyo Institute of Technology, Meguro Tokyo 152-8552, Japan
Correspondence to: R. Saito (E-mail: rsaito@polymer.titech.ac.jp)

ABSTRACT: Poly[6,6′-(1-methylethylidene)bis(3,4-dihydro-3-2H-1,3-hexylbenzoxazine)] (PB-hda)-silica nanocomposites were synthesized with perhydropolysilazane (PHPS) and PB-hda by ring opening polymerization in one step. Both high transparency and good water vapor barrier property (WVP) are required to be improved in the field of packing and electronic materials, such as OLED, solar cell, and electronic paper. PB-hda has shown high toughness and high thermal stability. However, it became dark brown and showed a reduction of WVP with increasing curing temperature, which make it difficult to be applied to packing and electronic materials. In this study, we aim to improve transparency and WVP by addition of PHPS into PB-hda matrix. It was found that nanocomposites showed the improvement of WVP and transparency owing to Si—O—C linkages between PB-hda and PHPS. In particular, a nanocomposite with 1 wt % of silica showed the most significant improvement in terms of transparency and the WVP. These properties were found to be influenced by the thickness of the combined polymer-silica layers that formed around the silica particles; these layers were thickest in the 1 wt % sample. © 2016 Wiley Periodicals, Inc. J. Appl. Polym. Sci. **2016**, *133*, 44238.

KEYWORDS: composites; films; nanostructured polymers; optical properties

Received 8 May 2016; accepted 27 July 2016
DOI: 10.1002/app.44238

INTRODUCTION

Polybenzoxazine is a new phenolic thermosetting resin, which is produced by ring opening polymerization of benzoxazine monomers.[1–5] It has several advantages over conventional thermosetting resins, such as molecular design flexibility,[6–9] no need for catalysts,[10] and high dimensional stability because of zero shrinkage during curing.[1,11–14]

6,6′-(1-methylethylidene)bis(3,4-dihydro-3-2H-1,3-hesylbenzoxazine (B-hda) is one such benzoxazine monomer that has been studied.[15] The chemical structures of B-hda and poly6,6′-(1-methylethylidene)bis(3,4-dihydro-3-2H-1,3-hesylbenzoxazine (PB-hda) are shown in Scheme 1. PB-hda has shown high toughness and high char yields even at 900 °C.[15] However, with increased curing temperature PB-hda films become dark brown and show poor transparency with increasing curing temperature. Water vapor barrier properties (WVPs) decreased with increasing curing temperatures because of the increase of hydroxy groups.[16]

In previous studies, we greatly improved the WVP by reacting the hydroxy groups of poly(tert-butyl-acrylate-*co*−2-hydroxyethyl methacrylate) and Si—H groups of perhydropolysilazane (PHPS).[17] Thus, we anticipate an improvement of the WVP in our PB-hda-silica nanocomposites because of the connections between the hydroxy groups of PB-hda and Si—H groups of PHPS. PB-hda's poor transparency is also expected to be improved owing to these chemical linkages.

PHPS, a silica precursor, has the repeating unit of SiH_2—NH. The chemical structure of PHPS is shown in Scheme 2.[18] PHPS is easily converted into silica at low temperatures under steam[19,20] unlike other silica precursors, such as orthosilicate and polyhedral oligomeric silsesquioxanes.[21,22] PHPS is soluble in many organic solvents such as chloroform, toluene, and xylene. It has also demonstrated good reactivity with hydroxy groups: an organic polymer with hydroxy groups can easily be used with PHPS to synthesize nanocomposites.[23–26]

In this work, we aim to improve both transparency and the WVP of PB-hda by incorporation of silica into the PB-hda matrix. The transparency of the nanocomposite films was measured by UV-vis spectroscopy, and their WVPs were measured using the cup method.

EXPERIMENTAL

Materials

2,2-Bis(4-hydroxyphenyl)propane (bisphenol A, TCI, > 99.0%), paraformaldehyde (TCI, > 90.0%), 1,6-diaminehexane (TCI, >99.0%), *p*-cresol (Wako, 99.0%), PHPS/dibutyl ether solution (NN-120, AZ Electronic Materials, 20 wt % of PHPS, number-

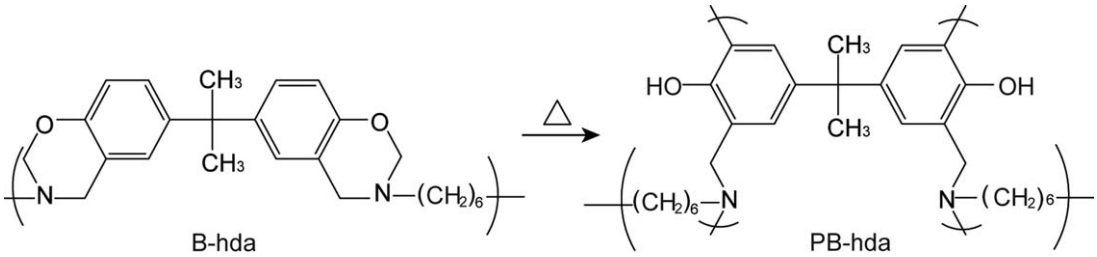

Scheme 1. The chemical structure of B-hda and PB-hda.

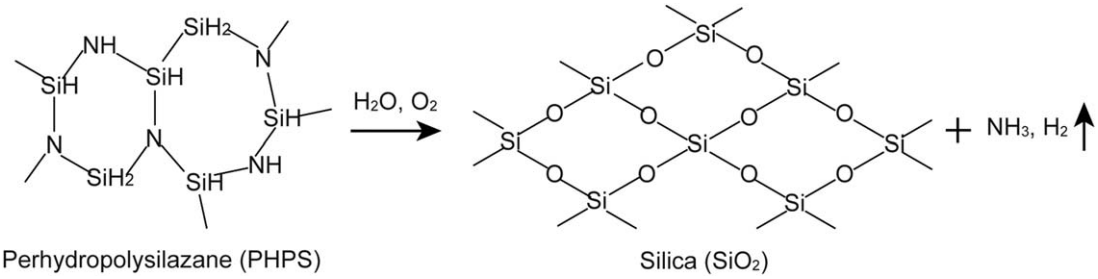

Scheme 2. The chemical structure of PHPS and its conversion to silica.

average molecular weight (M_n) = 700), sodium hydrogen carbonate (Kanto, 99%), sodium hydroxide (Kanto, 95%), anhydrous magnesium sulfate (Kanto, 95%), calcium chloride (Kanto, 90%), diethyl ether (Kanto, 99%), paraffin (Kanto, m.p: 60–62 °C), tetrahydrofuran (THF, Kanto, 99.5%), ethanol (Kanto, 99.5%), acetone (Kanto, 99.0%), toluene (Kanto, 99.0%), ammonia solution (Kanto, concn. 28.0 - 30.0%), hydrogen peroxide (Kanto, concn. 34.5%), deionized water, and chloroform-*d* ($CDCl_3$ with 0.03 v/v % TMS, ACROS, D > 99.8%) were used as received.

Synthesis of Polybenzoxazine-Silica Nanocomposites Films

6,6′(1-Methylethylidene)bis(3,4-dihydro-3-2H-1,3-hexylbenzoxazine) (B-hda) was synthesized based on the literature.[16] The specimens were prepared as follows. Teflon sheets with 7 cm in average diameter were prepared and overlaid with aluminum foil. Parting agent (Shin-Etsu Silicone, KE45T) was applied to aluminum foil and dried. NN-120 (0.37 mL) was dried under vaccum for 4 h. Then, a PHPS/THF solution was prepared by the addition of THF (0.14 mL) to the dried NN-120. B-hda (0.4 g) was dissolved in THF (3.6 mL). The PHPS/THF solution was added dropwise into the B-hda solution and stirred for 10 min under nitrogen flow. B-hda and PHPS mixture solution were cast on the sheets and gradually dried under nitrogen flow. The dried films were cured at 160 °C for 1 h and then cooled to room temperature. Aluminum foil was peeled off from the cured films and the films were cured at 200 °C for 1 h and 240 °C for 1 h with the insertion of the cured film at 160 °C between two glass plates. Then, the films were heated at 60 °C for 7 h with a small amount of water and dried at 40 °C for 14 h *in vacuo*. Figure 1 shows the formation of microphase-separated structure of PB-hda-silica nanocomposite cured at 240 °C.

Measurements

Ultraviolet Visible Spectroscopy (UV-vis). The transparency of the nanocomposites films were measured with a UV-vis spectrophotometer (JASCO V-530). PB-hda-silica nanocomposites films with 60–110 μm in thick were measured in a wavelength range from 400 to 1000 nm. Air was used as a reference.

Measurement of WVP. WVP was measured by the cup method with the cups of 6 cm in diameter and 1.5 cm in deep. The cups were placed in a desiccator with a saturated ammonium nitrate solution (56 ± 1.5 humidity [RH]) at 23.5 ± 1°C. The weight of cups was measured at 24 h intervals for 12 days.

RESULTS AND DISCUSSION

Transparency of Nanocomposites

In this work, PB-hda-silica nanocomposite films were prepared by ring opening polymerization in one step. Figure 2 shows PB-hda and PB-hda-silica nanocomposite samples with 12 wt % silica, which were prepared for the WVP measurement. All films

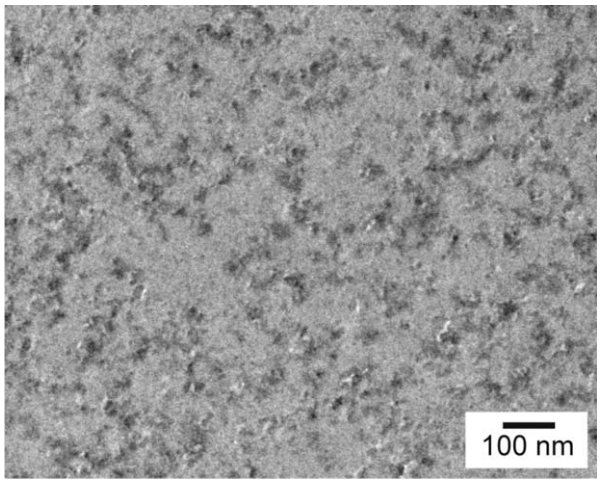

Figure 1. TEM image of cross-section of PB-hda-silica nanocomposites with 12 wt % of silica cured at 240 °C.[16]

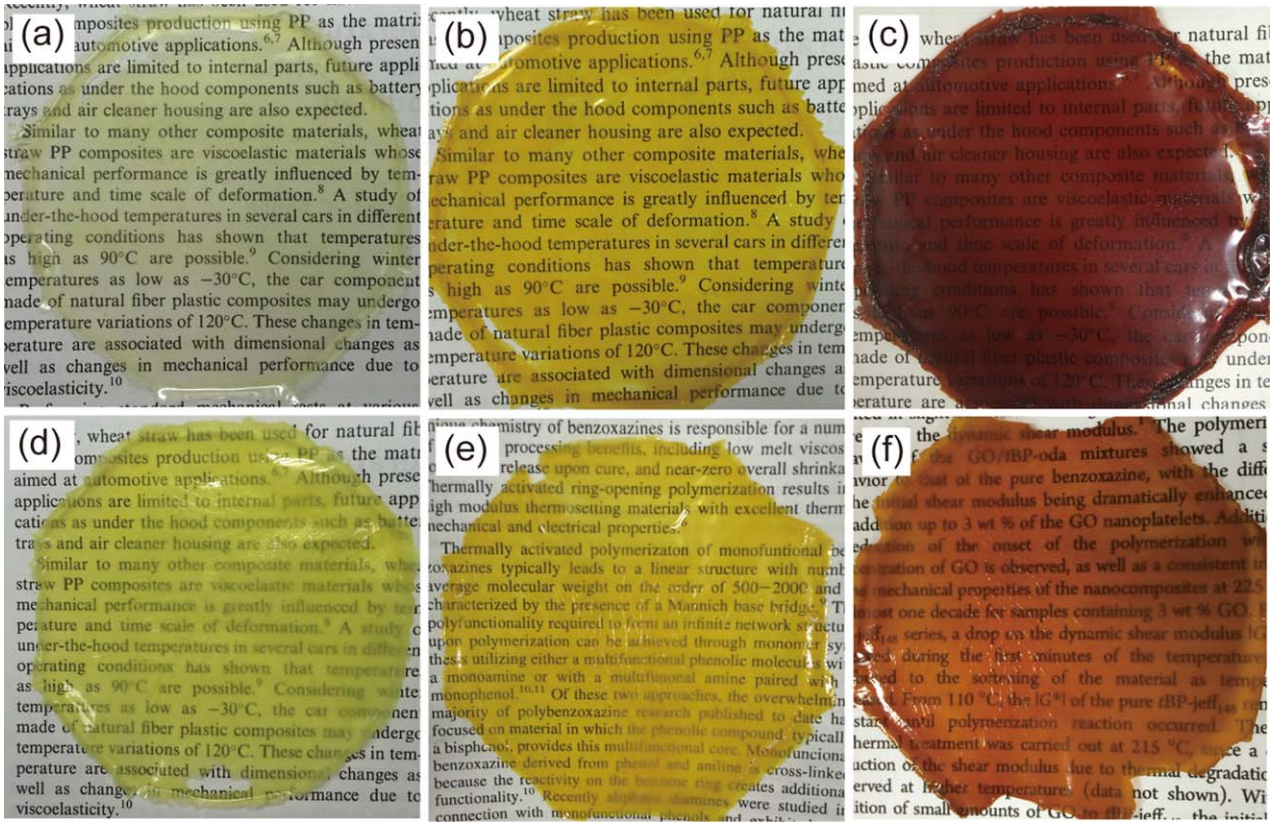

Figure 2. PB-hda and PB-hda-silica nanocomposites with 12 wt % silica for the measurement of WVP curing at 160 °C (a) and (d), 200 °C (b) and (e), and 240 °C (c) and (f). [Color figure can be viewed in the online issue, which is available at wileyonlinelibrary.com.]

darkened with increasing curing temperature. However, after curing at 240 °C, the nanocomposite film was lighter and more transparent than the PB-hda sample. This is because the chromogenic effect of benzene group would be suppressed by the formation of Si—O—C linkages between the hydroxy groups of PB-hda and the Si—H groups of PHPS form at high curing temperatures.[16]

To investigate the transparency of the nanocomposites, the transmittance of the samples was measured by UV-vis at 600 nm. Figure 3(a) shows UV-vis spectra of the films cured at 240 °C in a wavelength range from 400 to 1000. The transmittance at 600 nm shows the lowest value, 58%, in PB-hda, and nanocomposites show higher values. The thickness of the films was in a range from 60 to 110 μm. To neglect the effect of film

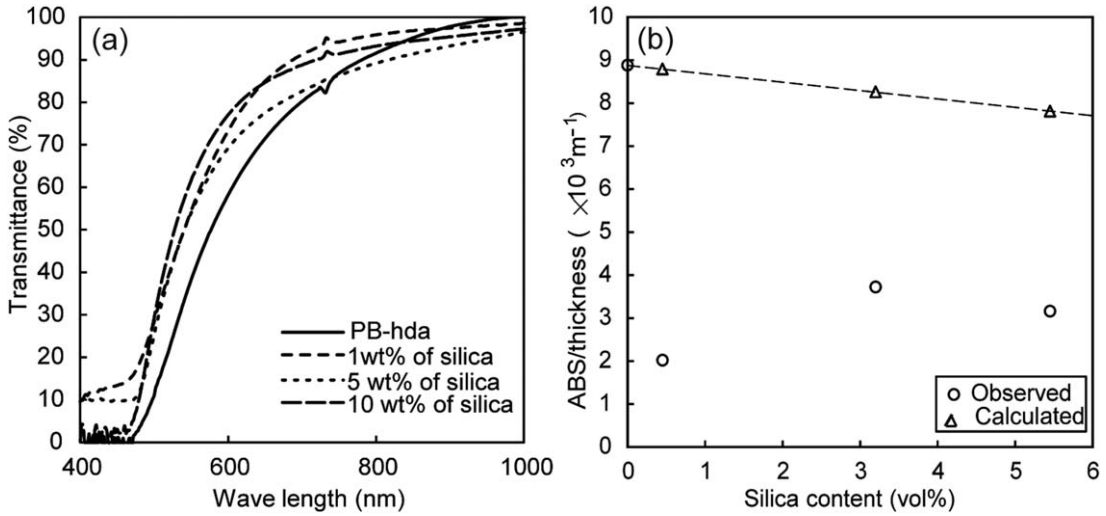

Figure 3. Transparency of PB-hda and PB-hda-silica nanocomposites at 600 nm. (a) transmittance of the samples and (b) the absorbance of the films per unit thickness and silica content.

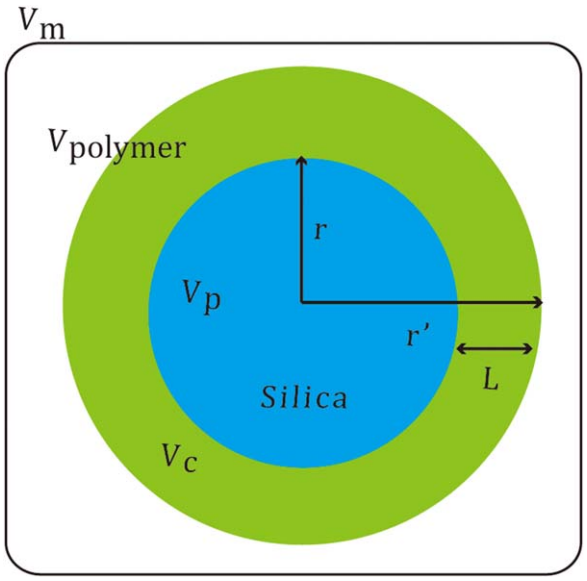

Figure 4. Schematic structure of molecular model of nanocomposites. [Color figure can be viewed in the online issue, which is available at wileyonlinelibrary.com.]

thickness, the absorbance of the film was corrected per unit thickness, m, by Lambert–Beer law. Figure 3(b) shows the absorbance of the films per unit thickness. The circles in Figure 3(b) are the observed values. The absorbance per thickness of PB-hda was 8.88×10^3 m^{-1} while the nanocomposites all displayed smaller values, that is, the nanocomposite films were more transparent than PB-hda. The silica provided by PHPS was highly transparent and microphase separation occurred in the nanocomposites. If the increased transparency of the nanocomposites were caused by PB-hda being diluted by silica, then it would have the following calculated absorbance, $A_{calc.}$:

$$A_{calc.} = A_{polymer} \times n_{polymer} \quad (1)$$

where $A_{polymer}$ is the absorbance per thickness of PB-hda and $n_{polymer}$ is the polymer volume fraction of PB-hda-silica nanocomposites. The $A_{calc.}$ values are represented by triangles in Figure 3(b). The $A_{calc.}$ values were higher than the observed ones. This suggests that in addition to polymer dilution, other mechanisms improve transparency.

In the observed values, the nanocomposite with 1 wt % of silica showed the lowest absorbance, 2.02×10^3 m^{-1}. Transparency of nanocomposites with 1 wt % of silica was improved the most in nanocomposites with all silica contents. We can assume that the chromogenic effect of benzene group would be suppressed by the formation of Si—O—C linkages between PB-hda and PHPS and have an influence on the transparency of the nanocomposites.

To further investigate this relationship between transparency and silica content, a molecular model was used to predict the sizes of domains in which the polymer was combined with silica. Figure 4 shows the structure on which the molecular model is based.[27] A spherical silica domain was assumed because the silica content values used were below 12 wt %, which is within the range for spherical domains to be formed in the microphase separation based on Molau's law.[28] Composite polymer-silica domains should, therefore, form layers of thickness L around these spherical silica particles. In Figure 4, V_m is defined as the unit cell volume of nanocomposites containing a spherical silica domain. Volume of the spherical silica domain V_p is calculated by $4\pi r^3/3$, where r is the radius of a spherical silica domain. Weight of a spherical silica domain, W_p, is calculated by dV_p, where d is the density of silica (2.2 g/cm^3). V_m is also expressed by eq. (2):

$$V_m = \frac{W_p}{S} \quad (2)$$

where S is the fraction of silica in the nanocomposite. The entire volume of the polymer in V_m, $V_{polymer}$, is calculated as follows:

$$V_{polymer} = V_m - V_p \quad (3)$$

$V_{polymer}$ contains the volume of the combined polymer V_c, which can be obtained from the weight fraction of polymer involved in the silica domain, W. From results of thermogravimetric analysis,[16] W was calculated using eq. (4).

$$W = \frac{\text{Char residue} - (\text{Weight fraction of silica in nanocomposite} + (\text{Weight fraction of polymer in nanocomposite}) \times Q)}{\text{Weight fraction of polymer in nanocomposite}} \times 100 \quad (4)$$

where Q is the char residue of PB-hda at 900 °C. Thus, W is expressed using V_c and $V_{polymer}$ as follows:

$$W = \frac{V_c}{V_{polymer}} \quad (5)$$

The volumes of the silica domain and the combined polymer are expressed in eq. (6) when the spherical silica domain is covered by the combined polymer. The total radius of a spherical domain containing silica and the combined polymer, r', is determined by eq. (7).

$$\frac{4\pi r'^3}{3} = V_c + V_p \quad (6)$$

$$r' = \left(\frac{3(V_c + V_p)}{4\pi}\right)^{\frac{1}{3}} \quad (7)$$

L is equal to $r' - r$.

Figure 5 shows the relationship between L and the absorbance of PB-hda-silica nanocomposites. The nanocomposite with 1 wt % of silica showed the largest L value, 15.5 nm, and the lowest

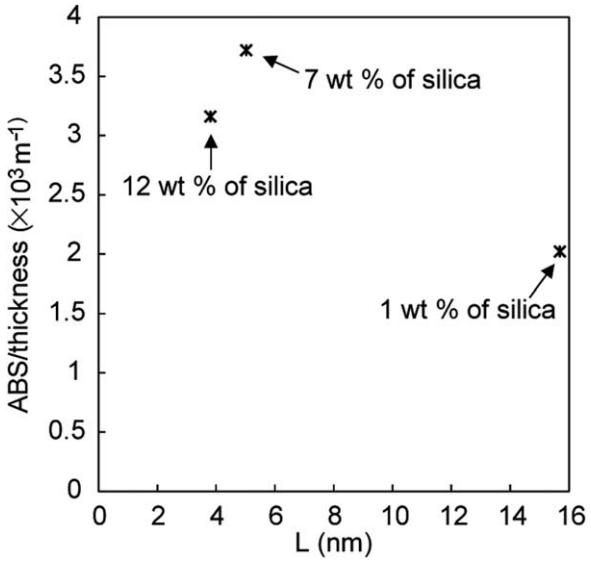

Figure 5. The relationship between thickness of combined polymer layer, *L* and the absorbance of PB-hda-silica nanocomposite.

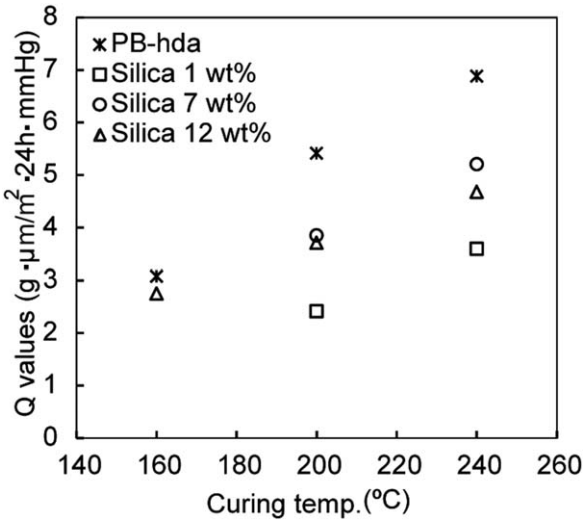

Figure 6. Curing temperature dependence of *Q* value of PB-hda and PB-hda-silica nanocomposites.

absorbance, 2.02×10^3 m^{-1}. Interestingly, *L* decreased with increasing silica content, while absorbances of the nanocomposites with 7 and 12 wt % of silica were higher than that of the nanocomposite with 1 wt % of silica. The chemical linkages between PB-hda and PHPS formed in the combined region, and the transparency of the nanocomposites was improved because these chemical linkages, which cause the chromogenic effect of the benzene group to be suppressed. Consequently, it was not the silica content but the effective formation of a com-

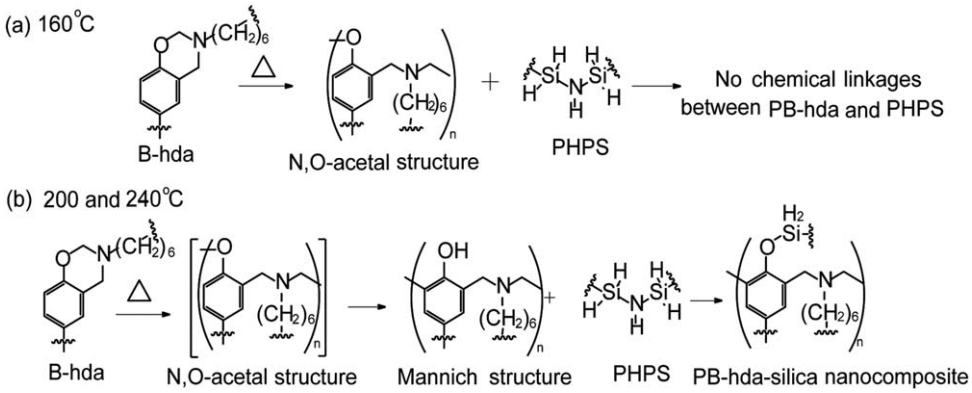

Figure 7. The reaction scheme to synthesize PB-hda-silica nanocomposites with different polymerization temperatures (a) 160 °C and (b) 200 and 240 °C.

Table I. The Thickness of Combined Polymer Layer, *L*, and the *Q* Value of PB-hda-Silica Nanocomposite Cured at 240 °C for 1 h

Code	B-hda (g)	THF[a] (mL)	PHPS (g)	NN-120[b] (mL)	THF[c] (mL)	PHPS (%)	Silica (%)	*Q* (g μm/m² 24 h mmHg)	*L* (nm)
PB-hda						—	—	6.21	—
PB-hda-PHPS 1	0.4	3.6	0.13	0.022	0.07	1	1	3.59	15.5
PB-hda-PHPS 2	0.4	3.6	0.24	0.04	0.06	5	7	5.21	5.03
PB-hda-PHPS 3	0.4	3.6	0.06	0.37	0.14	10	12	4.68	3.81

Curing condition: at 240 °C for 1 h.
[a] Solvent of B-hda.
[b] NN-120: a perhydropolysilazane (PHPS)/dibutyl ether solution with 20 wt % of PHPS.
[c] Solvent of PHPS.

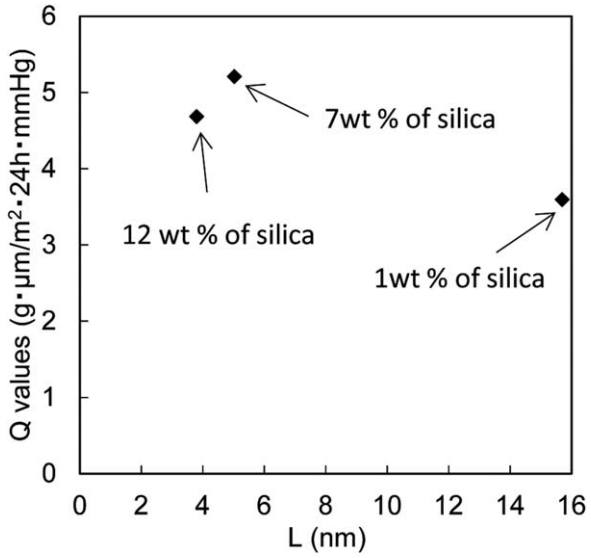

Figure 8. The relationship between thickness of combined polymer layer, *L*, and the *Q* value of PB-hda-silica nanocomposite cured at 240 °C for 1 h.

bined region with PB-hda and PHPS linkages that was the most important for improving transparency.

WVP of Nanocomposites

To investigate the WVPs of PB-hda and PB-hda-silica nanocomposites, permeability coefficients of the films, *Q*, were measured using the cup method. *Q* was calculated according to the following equation:

$$Q \text{ value} = \frac{\Delta W \times \sigma}{S \times 24 \ h \times p} \tag{8}$$

where ΔW is the weight of water vapor permeation, σ is the film thickness, *S* is the area of the film, and *p* is the saturated water vapor pressure.

Figure 6 shows the *Q* values of the polymer and nanocomposite films. In the case of PB-hda, the *Q* values increased with increasing curing temperature. The WVP of the films decreased with increasing curing temperature. This can be explained by considering the chemical structure of PB-hda. The molar fraction of the Mannich structure increased with increasing curing temperature; thus, the amount of hydroxy groups in PB-hda also increased. As a result, the diffusion of water vapor accelerated in films formed at higher temperatures. Conversely, for nanocomposite with 12 wt % of silica, the WVPs of nanocomposites cured at 200 and 240 °C were improved, while silica had no influence on the WVP of the nanocomposite cured at 160 °C.

Figure 7 shows the reaction scheme to synthesize of PB-hda-silica nanocomposites at different polymerization temperatures. It has been reported that the N,O-acetal structure was preferably formed by curing at low temperature, and then the N,O-acetal structure was rearranged to the Mannich structure over 200 °C.[29] The Si—O—C chemical linkages between the hydroxy groups of PB-hda and the Si—H groups of PHPS were not formed when curing at 160 °C. At 160 °C, only the N,O-acetal structure, which was hydrophobic due to the lack of hydroxy group, was formed. Therefore, the WVP at 160 °C was low without PHPS and was not improved by the addition of PHPS into polymer matrix. Conversely, the Mannich structures were formed at 200 and 240 °C; thus, the hydroxy groups of PB-hda and Si—H groups of PHPS were competitively reacted and Si—O—C chemical linkages were formed by curing at 200 and 240 °C, which leads to the decrease of the amount of hydroxy groups in the film. As a result, the reduction of the WVP of PB-hda at higher curing temperatures was improved by the addition of PHPS. To summarize, when the nanocomposite and PB-hda were synthesized at 200 and 240 °C, the *Q* values decreased. In particular, nanocomposites with 1 wt % of silica cured at 200 and 240 °C showed the lowest *Q* values of all nanocomposites, which demonstrates that the WVP of the nanocomposite with 1 wt % of silica improved the most. This phenomenon can also be explained by the fact that the nanocomposites with 1 wt % of silica exhibit the largest *L* values.

The *L* and *Q* values were listed in Table I. Figure 8 shows the relationship between the *L* and *Q* values of the various nanocomposites cured at 240 °C for 1 h. The lowest *Q* value, 3.59 g μm/m²·24 h·mmHg, correlated with the largest *L* value, 15.5 nm, for the sample with 1 wt % of silica. When *L* decreased with increasing silica content, *Q* increased. The WVP was most improved in the sample with the highest *L* value.

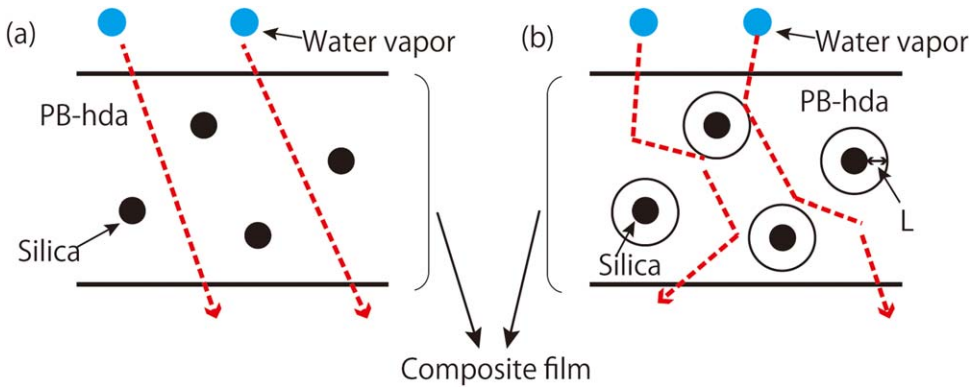

Figure 9. Schematic structures of the path of water vapor of the cross-section of nanocomposite film with 1 wt % of silica without taking account of *L* (a), and with taking account of *L* (b). [Color figure can be viewed in the online issue, which is available at wileyonlinelibrary.com.]

Figure 9(a) is a cross sectional diagram of the nanocomposite film illustrating the paths water vapor. Generally, the WVP increases with increasing silica content owing to the increased water vapor path lengths. Interestingly, water vapor path lengths in the nanocomposite with 1 wt % of silica drastically increased because of the sample's large L value, as illustrated in Figure 9(b). When the amount of PHPS was small, the reaction between the polymer and PHPS increased and molecular dispersion of silica occurred within the polymer matrix. Therefore, it was hard for the silica particles to aggregate in the nanocomposite film and large domains of the combined polymer-silica formed in layers around the spherical silica particles. Consequently, the WVP of the nanocomposites was the most drastically improved in the 1 wt % of silica sample.

CONCLUSIONS

PB-hda-silica nanocomposite films were prepared by ring opening polymerization in one step. Transparency was improved owing to the formation of Si—O—C linkages and suppression of the chromogenic effect of the benzene group. The WVP was also improved by incorporation of silica in the PB-hda matrix at high curing temperatures because of the formation of Si—O—C linkages—although the pure polymer films cured at 240 °C showed the highest Q values because they also contained the highest concentrations of hydroxy groups. We found that both the WVP and transparency were improved by the thickness increase of the combined polymer-silica layer around the silica particles (L), rather than by increases in the silica content.

ACKNOWLEDGMENTS

This work was supported by a Grant-in-Aid for Scientific Research on Innovative Areas "New Polymeric Materials Based on Element-Blocks (No. 2401)" (JSPS KAKENHI Grant Number JP15H00727)

REFERENCES

1. Ishida, H.; Low, H. Y. *Macromolecules* **1997**, *30*, 1099.
2. Shen, S. B.; Ishida, H. *Polym. Sci. Part B* **1999**, *37*, 3257.
3. Macko, J. A.; Ishida, H. *Polymer* **2001**, *42*, 227.
4. Agag, T.; Takeichi, T. *Macromolecules* **2003**, *36*, 6010.
5. Takeichi, T.; Agag, T.; Rachib, Z. *J. Polym. Sci., Part A: Polym. Chem.* **2001**, *39*, 2633.
6. Chernykh, A.; Agag, T.; Ishida, H. *Polymer* **2009**, *50*, 382.
7. Ning, X.; Ishida, H. *J. Polym. Sci., Part B: Polym. Phys.* **1994**, *32*, 921.
8. Kim, H. J.; Brunovska, Z.; Ishida, H. *Polymer* **1999**, *40*, 1815.
9. Hao, G.-P.; Li, W.-C.; Qian, D.; Wang, G.-H.; Zhang, W.-P.; Zhang, T.; Wang, A.-Q.; Schüth, F.; Bongard, H.-J.; Lu, A.-H. *J. Am. Chem. Soc.* **2011**, *133*, 11378.
10. Takeichi, T.; Komiya, I.; Takayama, Y. *Kyoka-Purasutikkus* **1997**, *43*, 109.
11. Ning, X.; Ishida, H. *J. Polym. Sci., Part A: Polym. Chem.* **1994**, *32*, 1121.
12. Ishida, H.; Allen, D. *J. Polym. Sci., Part B: Polym. Phys.* **1996**, *34*, 1019.
13. Wirasate, S.; Dhumrong varaporn, S.; Allen, D.; Ishida, H. *J. Appl. Polym. Sci.* **1998**, *70*, 1299.
14. Ishida, H.; Allen, D. *J. Appl. Polym. Sci.* **2001**, *79*, 406.
15. Takeichi, T.; Takuya, K.; Agag, T. *Polymer* **2005**, *46*, 12172.
16. Lee, J. Y.; Takeichi, T.; Saito, R. *Polymer* **2016**, *99*, 536.
17. Saito, R.; Nakagawa, D. *Polym. Adv. Technol.* **2009**, *20*, 285.
18. Prager, L.; Dierdorf, A.; Liebe, H.; Naumov, S.; Stojanović, S.; Heller, R.; Wennrich, L.; Buchmeiser, M. R. *A Euro J. Chem.* **2007**, *13*, 8522.
19. Low, M. J. D.; Severdia, A. G. *J. Colloid Interface Sci.* **1982**, *86*, 111.
20. Severdia, A. G.; Low, M. J. D. *Langmuir* **1988**, *4*, 1234.
21. Agag, T. *Mater. Sci. Forum* **2004**, *449–452*, 1157.
22. Low, M. J. D.; Severdia, A. G. *J. Colloid Interface Sci.* **1982**, *86*, 1.
23. Saito, R.; Kuwano, K.; Tobe, T. *J. Macromol. Sci. Pure Appl. Chem.* **2002**, *A39*, 171.
24. Saito, R.; Mori, Y. *J. Macromol. Sci. Pure Appl. Chem.* **2002**, *A 39*, 915.
25. Mori, Y.; Saito, R. *J. Macromol. Sci. Pure Appl. Chem.* **2003**, *A 40*, 671.
26. Saito, R.; Kobayashi, S.-I.; Hosoya, T. *J. Appl. Polym. Sci.* **2005**, *97*, 1835.
27. Zeng, Q. H.; Yu, A. B.; Lu, G. Q. *Prog. Polym. Sci.* **2008**, *33*, 191.
28. Molau, G. E. Block Polymers; Plenum Press: New York, **1970**.
29. Liu, C.; Shen, D.; Sebastián, R. M.; Marquet, J.; Schönfeld, R. *Macromolecules* **2011**, *44*, 4616.